bioRxiv preprint doi: https://doi.org/10.1101/143768; this version posted May 30, 2017. The copyright holder for this preprint (which was not certified by peer review) is the author/funder, who has granted bioRxiv a license to display the preprint in perpetuity. It is made available under aCC-BY 4.0 International license.

Precentral gyrus abnormal connectivity in male and female schizophrenia patients

Mahdi Zarei*

University of California, San Francisco

Abstract

The present study demonstrates the Precentral gyrus (PreCG) alteration and its abnormal connectivities in Schizophrenia (SCH) patients. The resting-sate functional magnetic resonance imaging (rs-fMRI) data of healthy control subjects and SCH patients (Centre for Biomedical Research Excellence data set) are used to examine the aberrant functional brain connectome in SCH which contains raw anatomical and functional MR data from 72 patients with Schizophrenia and 75 healthy controls, ranging in age from 18 to 65 years old. Our results show that PreCG has abnormal communication with Thalamus, Hippocampus, Parahippocampal Gyrus (pPaHC), posterior division of Supramarginal Gyrus (pSMG) and medial prefrontal cortex (mPFC) (p-FDR=0.05).

1 Introduction

Recent studies shows that Precentral gyrus (PreCG) has significant reduced of functional activity (FC) in Schizophrenia (SCH) patients [16, 13]. Also, SCH is associated with volume deficits in Precentral gyrus [15]. Another research indicates that the patients with SCH showed lower activation in left PreCG than right PreCG [10] and a regional homogeneity (ReHo) study showed decreased ReHo in right Precentral gyrus [19].

In this research we examined the PrecG functional connectivity impairment in SCH patients using ROI based analysis [14]. We used the Center for Biomedical Research Excellence data set (COBRE) ([8]) to demonstrate how the functional connectivity of the PreCG with the rest of the brain regions changes in SCH. In conjunction with previous studies, our results indicate that the PreCG has abnormal connectivity with some of the brain regions like Thalamus and Hippocampus, but dis impairments are not the similar in two hemisphere. We also analyzed the FC differences between male and female SCH patients and showed that the regions like Thalamus are more affected in the female SCH patients.

2 Data

We included 48 subjects from Centre for Biomedical Research Excellence COBRE data set; 24 healthy controls and 24 schizophrenia patients (12 men and 12 women in each group) in the study. In the original data set (see table 2) there are more male subjects than females and to allow the same effects of the both genders in the results we used the above arrangement. COBRE data contains raw anatomical and functional MRI data from patients with Schizophrenia and healthy controls. Some papers that by the COBRE group published based on this data [11, 17, 3]. This data set is available on [8] and contains raw anatomical and functional MR data from patients with Schizophrenia and healthy controls, ranging in age from 18 to 65 years old. Resting fMRI, anatomical MRI, phenotypic data for every participant including: gender, age, handedness and diagnostic information are released.

*Electronic address: Mahdi.Zarei@ucsf.edu, mehdi.nn@gmail.com

bioRxiv preprint doi: https://doi.org/10.1101/143768; this version posted May 30, 2017. The copyright holder for this preprint (which was not certified by peer review) is the author/funder, who has granted bioRxiv a license to display the preprint in perpetuity. It is made available under aCC-BY 4.0 International license.

	N	Age(SD)	%Female	%Right-Handed
Schizophrenia	72	38.16(13.89)	0.19	0.83
Patients	74	35.82(11.58)	0.31	0.96

Table 1: Demographic characteristics of subjects in COBRE data [1]

3 Analysis

Different preprocessing methods like realignment, coregistering, normalization are applied for the structural and functional data. The functional volumes are coregistered with the region of interest and structural volumes. Regions of interest and all the Brodmann areas defined from Talairach daemon assigned to all subjects. By segmentation of structural image for each subject, grey matter, white matter and cerebrospinal fluid (CSF) masks generated. Here, the time series of interest are the number of PCA components.

3.1 First and second level of covariates

In this step the realignment parameters in BOLD model is defined (first level covariate), then in the second level covariate the group level regressor is performed. We categorized the data input data into 4 groups; Control females, Control males, Patient females and Patient male.

After defining the experiment data, the functional data is imported, then the structural data is segmented to define the grey matter, white matter, cerebrospinal fluid region of interest. By performing PCA on within region of interests the ROIs time series is extracted.

4 Denoising of the data

Before analyzing the data we need to explore and remove the confounds. Different source of possible confounds like cerebrospinal fluid and white matter signal and within-subject covariate (realignment parameters) are considered. We chose the 5 dimension that is the number of temporal components are being used. Similarly, the number of dimension for white matter was 5 and the derivative order was 0 and the histogram plot r value before and after confound removal and the band-pass filter is set to [0.008 0.09]. Figure 4 (a and b) shows variance explained (r-square) by each of the possible confounding sources and the histogram plot at the center displays the voxel-to-voxel connectivity (r values) before, and after confound removal for 2 subjects. The histograms r-square in order to identify outlier subject and the quality control is computed for every subject (figure 4 c).

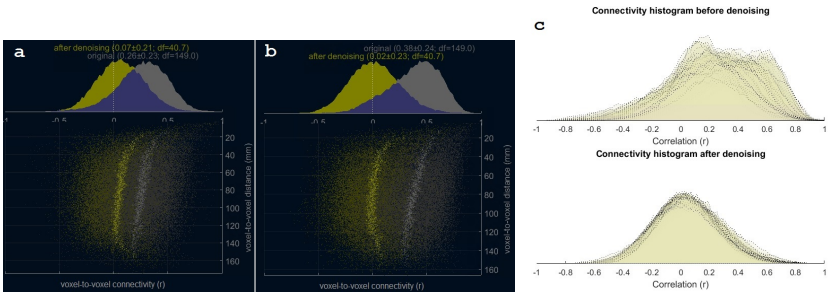

Figure 1: Histogram of functional connectivity values (r). Total variance explained (r-square) by each of the possible confounding sources for 2 subjects.

The functional connectivity (CONN) and Statistical Parametric Mapping (SPM) toolboxes [18, 5] used for spatially preprocessing (Realignment, coregistering, normalization) of structural and functional data of functional data is done using SPM toolbox. The functional volumes are coregistered with the region of interest and structural volumes. ROI-to-ROI correlational analysis were carried out by the CONN toolbox and SPM8. The preprocessing of the functional images considered of band-pass filtering of 0.008 - 0.09 Hz, motion correction, registration to structural images and spatial normalization to the MNI template. Then to reduce the physiological noise source, a Component Based Noise Correction Method (CompCor) has been used [2]. CompCor can

bioRxiv preprint doi: https://doi.org/10.1101/143768; this version posted May 30, 2017. The copyright holder for this preprint (which was not certified by peer review) is the author/funder, who has granted bioRxiv a license to display the preprint in perpetuity. It is made available under aCC-BY 4.0 International license.

be used for the reduction of noise in both blood oxygenation level dependent and perfusion-based functional magnetic resonance imaging data. False discovery rate correction is used to multiple hypothesis testing. Number of PCA components to be extracted for each ROI is set to one. It means that the time-series of interest is defined as the average BOLD activation within the ROI voxels, but it's possible to define it as the principal eigenvariates of the time-series within the ROI voxels. Regions of interest and all the Brodmann areas defined from Talairach daemon assigned to all subjects. By segmentation of structural image for each subject, grey matter, white matter and cerebrospinal fluid (CSF) masks were generated.

Bivariate correlation is used as a functional connectivity measures between two areas. General linear model (GLM) [12] used for comparison of connectivity results between genders and between control and Schizophrenia patients.

4.1 ROI based analysis

We investigated the hypothesis of connectivity differece in schizophrenia and used ROI analysing for the PreCG region of the brain. Two-sample t-test analyses computed via SPM8 [6] to compare the connectivity results of patients vs. controls and male patient vs. women patient to compare the connectivity across two group. Connectivity values (Fisher-transformed correlation coefficients) between the seed and the identified ROI was extracted from the connectivity map. Different source of interest can be defined for analyzing. Figure **??** shows the results connectivity analyzing based left primary somatosensory cortex and left associative visual cortex for subject 40121 from COBRE data that voxels with correlation coefficient 0.5 are colored.

4.2 First level voxel-based analysis

For a subject or condition it is possible to perform voxel-to-voxel analyzing that applies matrix of voxel-to-voxel connectivity values and there is no need for priori region of interest or seed analysis. In this method we can investigate whole brain connectivity. The voxel based analyzing can be based on connectivity pattern (Principal Component Analysis) between a voxel and the rest of the brain (*MVPA*). Another voxel based measeure is avialable in CONN toolboxes is *Indexes* that calculates the the average local connectivity between each voxel and its neighbors (Integrated Local Correlation) [4] or instead of average, the spatial asymmetry of the local connectivity can be used (Radial Correlation Contrast) [7]. Also, instead of local connectivity, global connectivity pattern between a voxel and the rest of the brain can be used (e.g. Radial Similarity Contrast) [9]. More details about measuring the Index can be found in [18].

5 Second level analysis

In the second level analysis step the between-subject contrast can be consider (e.g. to compared different groups like male vs. femals to see main effects in the connectivity within each group). In the ROI-to-ROI analyses, the first-level connectivity-measure matrix is used and the results can be thresholded at the desired p-value threshold. In this step by graph theoretical analyzing method provides the network measures like efficiency, centrality, and cost/degree to test the between-subject contrast.

6 Results

The connectivity contrast values between the PerCG right and the targets shows that the PreCG has abnormal communication with Thalamus, Hippocampus, Parahippocampal Gyrus (pPaHC), posterior division of Supramarginal Gyrus (pSMG) and medial prefrontal cortex (mPFC) (p-value=0.05). Figure 6 shows ROI-level results for PrecG left and right PreCG. Effects size for each region is shown by the dot size.

Functional connectivity difference of the left and right PreCG between healthy controls and SCH patients (controls>Schizophrenia) shows that the Connectivity of the left Hippocampus with both left and right PreCG decreased in SCH. More details about the the connectivity impairment of PreCG and the rest of the brain is demonstrated in figure 6. We also compaired SCH effects the PreCG in the mail and female patients (figure 6).

bioRxiv preprint doi: https://doi.org/10.1101/143768; this version posted May 30, 2017. The copyright holder for this preprint (which was not certified by peer review) is the author/funder, who has granted bioRxiv a license to display the preprint in perpetuity. It is made available under aCC-BY 4.0 International license.

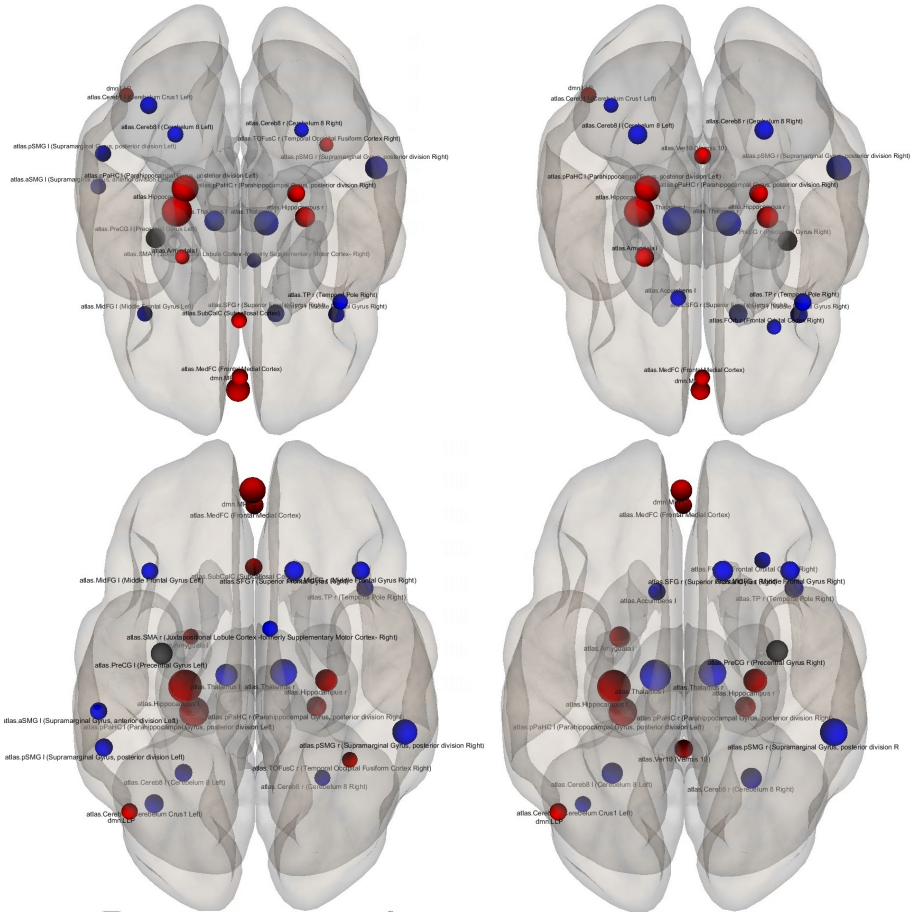

Figure 2: The superior (top) and the posterior views of the ROI-level results for each target ROI. The selected sources (precentral gyrus left and right) are shown by black dots and the targets are blue (control > SCH) and red (control < SCH). Effects size for each region is shown by the dot size.

7 Conclusion

Here, we investigate abnormal connectivities of left and right precentral gyrus in male and female Schizophrenia patients. Region of interest based analysis carried out for the healthy control and Schizophrenia patient data. To do this resting state functional magnetic resonance imaging data of healthy control subjects and SCH patients from Center for Biomedical Research Excellence are used to examine the aberrant functional brain connectome in Schizophrenia which contains raw anatomical and functional MR data from 72 patients with Schizophrenia and 75 healthy controls, ranging in age from 18 to 65 years old. We can summarize our results as follows:

- The precentral gyrus has abnormal communication with Thalamus, Hippocampus, Parahippocampal Gyrus (pPaHC), posterior division of Supramarginal Gyrus (pSMG) and medial prefrontal cortex (mPFC) (p-value=0.05).
- The right precentral gyrus has unusual connectivities with Hippocampus l, pPaHC l Thalamus l, Thalamus r and pSMG r.
- The right precentral gyrus has unbalanced connectivities with Hippocampus l, pPaHC l, Thalamus r, MPFC, pSMG r, Hippocampus r and Thalamus l.
- The connectivity impairments of the PreCG in SCH are different for male and female patients.

PreCG Precentral Gyrus pPaHC Parahippocampal Gyrus, posterior division MPFC The medial prefrontal cortex pSMG Supramarginal Gyrus, posterior division

bioRxiv preprint doi: https://doi.org/10.1101/143768; this version posted May 30, 2017. The copyright holder for this preprint (which was not certified by peer review) is the author/funder, who has granted bioRxiv a license to display the preprint in perpetuity. It is made available under aCC-BY 4.0 International license.

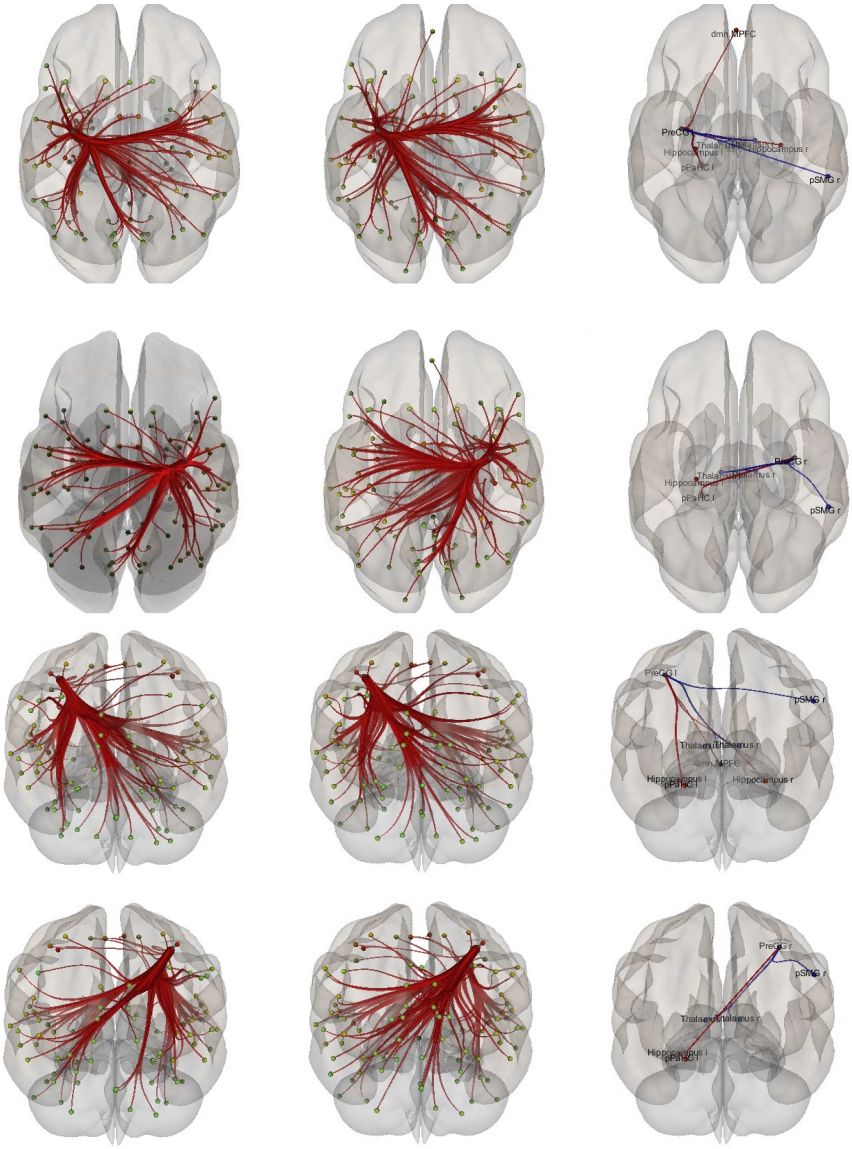

Figure 3: Functional connectivity difference of the left and right precentral gyrus between healthy controls vs. SCH patients (controls>Schizophrenia). The PrecG connectivity inthe healthy control, SCH patients and their difference are shown in the first, second and the last column respectively and the two top raws are the superior views and the the two bottom raws are the posterior views.

Table 2: The connectivity contrast values between the PerCG right and the targets (p-value=0.05) (the complete list of the effect size is provided in the supplementary data)

Analysis Unit	Statistic	p-unc	p-FDR
Seed Intensity = 18.77, Size = 5	PreCG r	F(30)(113) = 3.17	0.0000
PreCG r -Hippocampus l	T(142) = 4.16	0.0001	0.0074
PreCG r -Thalamus l	T(142) = -3.92	0.0001	0.0093
PreCG r -pPaHC l	T(142) = 3.62	0.0004	0.0151
PreCG r -Thalamus r	T(142) = -3.54	0.0005	0.0151
PreCG r -pSMG r	T(142) = -3.53	0.0006	0.0151

bioRxiv preprint doi: https://doi.org/10.1101/143768; this version posted May 30, 2017. The copyright holder for this preprint (which was not certified by peer review) is the author/funder, who has granted bioRxiv a license to display the preprint in perpetuity. It is made available under aCC-BY 4.0 International license.

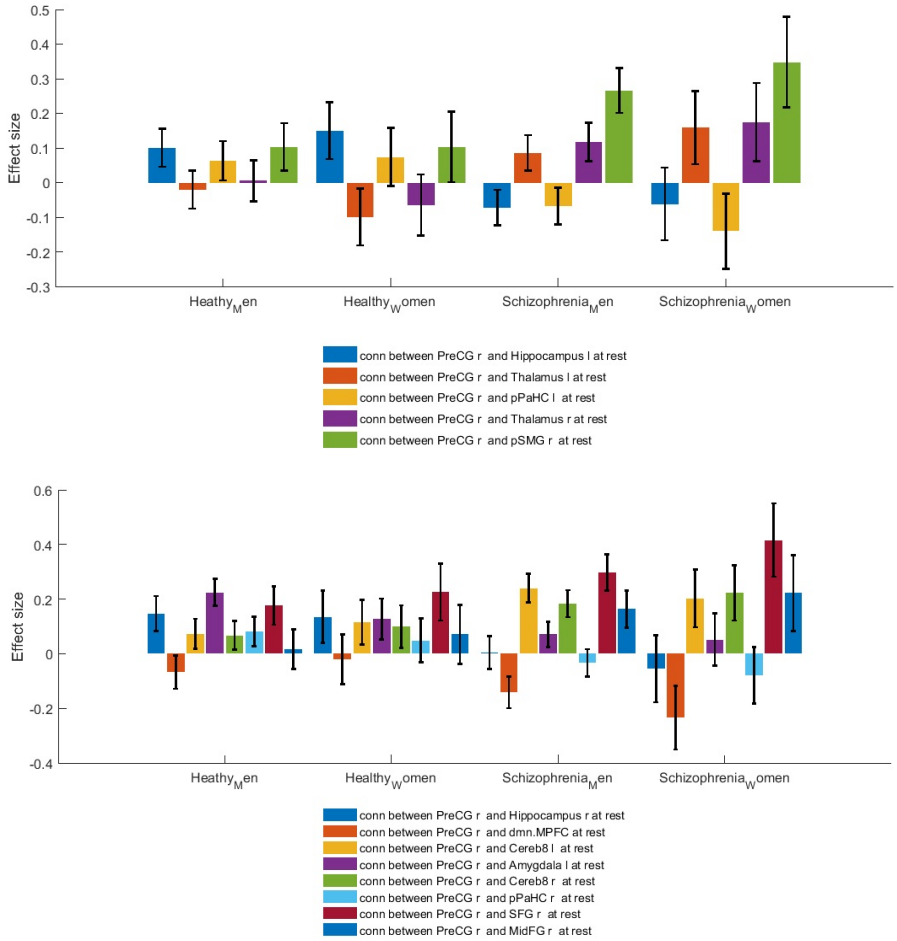

Figure 4: Functional connectivity difference of the ... precentral gyrus between healthy controls vs. SCH patients (controls>Schizophrenia).

Table 3: The connectivity contrast values between the PerCG left and the targets (p-value=0.05) (the complete list of the effect size is provided in the supplementary data)

Analysis Unit	Statistic	p-unc	p-FDR
Seed Intensity = 25.55, Size = 7	PreCG l	F(30)(113) = 3.41	0.0000
PreCG l -Hippocampus l	T(142) = 4.47	0.0000	0.0022
PreCG l -pPaHC l	T(142) = 4.02	0.0001	0.0063
PreCG l -Thalamus r	T(142) = -3.72	0.0003	0.0128
PreCG l -dmn.MPFC	T(142) = 3.64	0.0004	0.0131
PreCG l -pSMG r	T(142) = -3.48	0.0007	0.0179
PreCG l -Hippocampus r	T(142) = 3.12	0.0022	0.0450
PreCG l -Thalamus l	T(142) = -3.10	0.0023	0.0450

bioRxiv preprint doi: https://doi.org/10.1101/143768; this version posted May 30, 2017. The copyright holder for this preprint (which was not certified by peer review) is the author/funder, who has granted bioRxiv a license to display the preprint in perpetuity. It is made available under aCC-BY 4.0 International license.

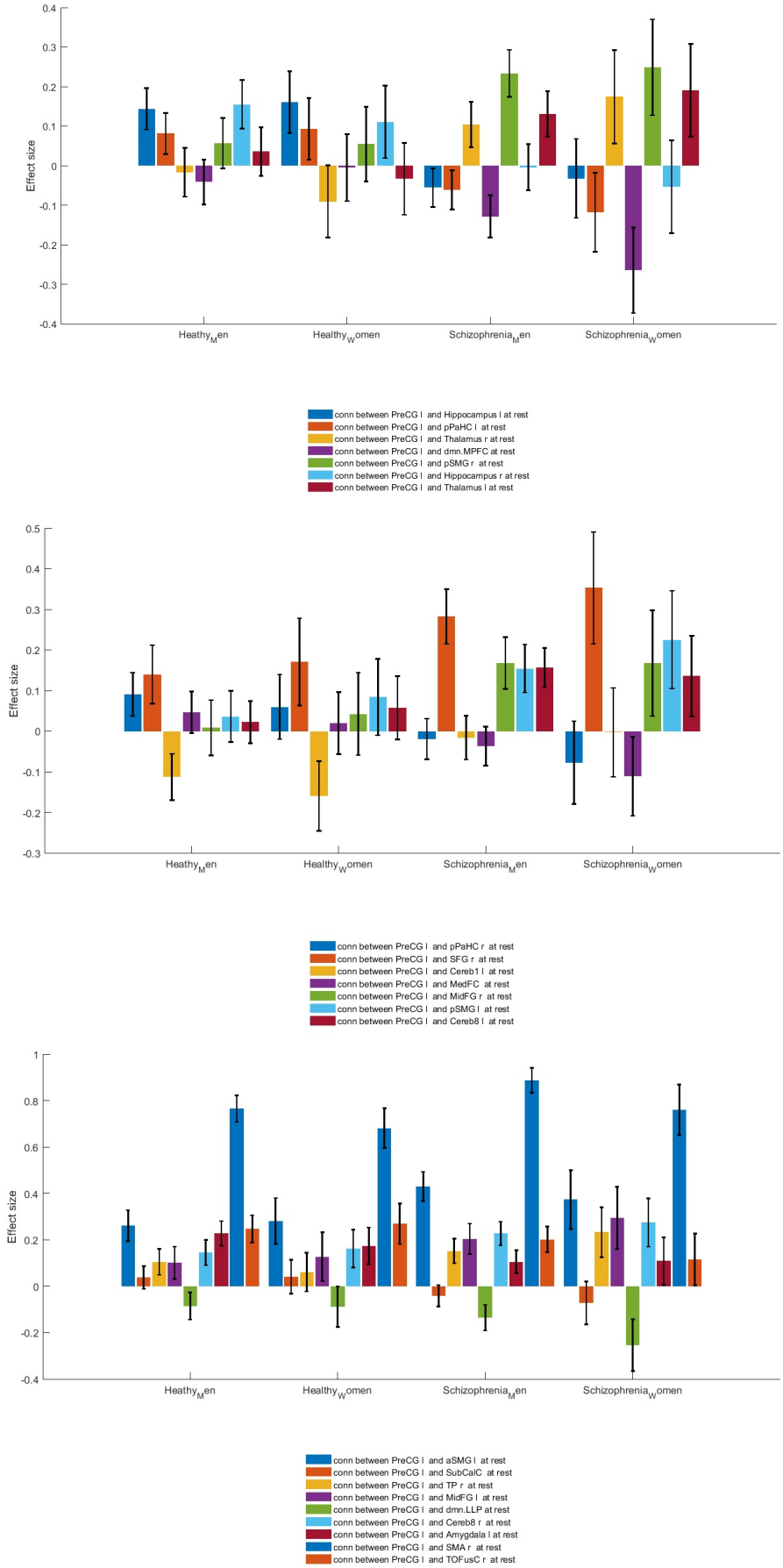

Figure 5: Functional connectivity difference of the ... precentral gyrus between healthy controls vs. SCH patients (controls>Schizophrenia).

bioRxiv preprint doi: https://doi.org/10.1101/143768; this version posted May 30, 2017. The copyright holder for this preprint (which was not certified by peer review) is the author/funder, who has granted bioRxiv a license to display the preprint in perpetuity. It is made available under aCC-BY 4.0 International license.

References

[1] Anderson, A., and Cohen, M. S. Decreased small-world functional network connectivity and clustering across resting state networks in schizophrenia: an fmri classification tutorial. *Frontiers in Human Neuroscience 7* (2013).

[2] Behzadi, Y., Restom, K., Liau, J., and Liu, T. T. A component based noise correction method (compcor) for bold and perfusion based fmri. *Neuroimage 37*, 1 (2007), 90–101.

[3] Calhoun, V. D., Sui, J., Kiehl, K., Turner, J., Allen, E., and Pearlson, G. Exploring the psychosis functional connectome: aberrant intrinsic networks in schizophrenia and bipolar disorder. *Frontiers in Psychiatry 2* (2011).

[4] Deshpande, G., LaConte, S., Peltier, S., and Hu, X. Integrated local correlation: a new measure of local coherence in fmri data. *Human Brain Mapping 30*, 1 (2009), 13–23.

[5] Friston, K. J. Functional and effective connectivity in neuroimaging: a synthesis. *Human Brain Mapping 2*, 1-2 (1994), 56–78.

[6] Friston, K. J. Functional and effective connectivity: a review. *Brain Connectivity 1*, 1 (2011), 13–36.

[7] Goelman, G. Radial correlation contrast—a functional connectivity mri contrast to map changes in local neuronal communication. *Neuroimage 23*, 4 (2004), 1432–1439.

[8] http://fcon _1000.projects.nitrc.org/indi/retro/cobre.html.

[9] Kim, J.-H., Lee, J.-M., Jo, H. J., Kim, S. H., Lee, J. H., Kim, S. T., Seo, S. W., Cox, R. W., Na, D. L., Kim, S. I., et al. Defining functional sma and pre-sma subregions in human mfc using resting state fmri: functional connectivity-based parcellation method. *Neuroimage 49*, 3 (2010), 2375–2386.

[10] Li, H.-j., Chan, R. C., Gong, Q.-y., Liu, Y., Liu, S.-m., Shum, D., and Ma, Z.-l. Facial emotion processing in patients with schizophrenia and their non-psychotic siblings: a functional magnetic resonance imaging study. *Schizophrenia research 134*, 2 (2012), 143–150.

[11] Mayer, A. R., Ruhl, D., Merideth, F., Ling, J., Hanlon, F. M., Bustillo, J., and Cañive, J. Functional imaging of the hemodynamic sensory gating response in schizophrenia. *Human Brain Mapping 34*, 9 (2013), 2302–2312.

[12] McCullagh, P. Generalized linear models. *European Journal of Operational Research 16*, 3 (1984), 285–292.

[13] Mubarik, A., and Tohid, H. Frontal lobe alterations in schizophrenia: a review. *Trends in Psychiatry and Psychotherapy 38*, 4 (2016), 198–206.

[14] Poldrack, R. A. Region of interest analysis for fmri. *Social cognitive and affective neuroscience 2*, 1/4 (2007), 67.

[15] Shepherd, A. M., Quidé, Y., Laurens, K. R., O'Reilly, N., Rowland, J. E., Mitchell, P. B., Carr, V. J., and Green, M. J. Shared intermediate phenotypes for schizophrenia and bipolar disorder: neuroanatomical features of subtypes distinguished by executive dysfunction. *Journal of psychiatry & neuroscience: JPN 40*, 1 (2015), 58–68.

[16] Singh, S., Goyal, S., Modi, S., Kumar, P., Singh, N., Bhatia, T., Deshpande, S. N., and Khushu, S. Motor function deficits in schizophrenia: an fmri and vbm study. *Neuroradiology 56*, 5 (2014), 413–422.

[17] Stephen, J. M., Coffman, B. A., Jung, R. E., Bustillo, J. R., Aine, C. J., and Calhoun, V. D. Using joint ica to link function and structure using meg and dti in schizophrenia. *NeuroImage 83* (2013), 418–430.

[18] Whitfield Gabrieli, S., and Nieto Castanon, A. Conn: a functional connectivity toolbox for correlated and anticorrelated brain networks. *Brain Connectivity 2*, 3 (2012), 125–141.

bioRxiv preprint doi: https://doi.org/10.1101/143768; this version posted May 30, 2017. The copyright holder for this preprint (which was not certified by peer review) is the author/funder, who has granted bioRxiv a license to display the preprint in perpetuity. It is made available under aCC-BY 4.0 International license.

[19] Xiao, B., Wang, S., Liu, J., Meng, T., He, Y., and Luo, X. abnormalities of localized connectivity in schizophrenia patients and their unaffected relatives: a meta-analysis of resting-state functional magnetic resonance imaging studies. *Neuropsychiatric Disease and Treatment 13* (2017), 467.

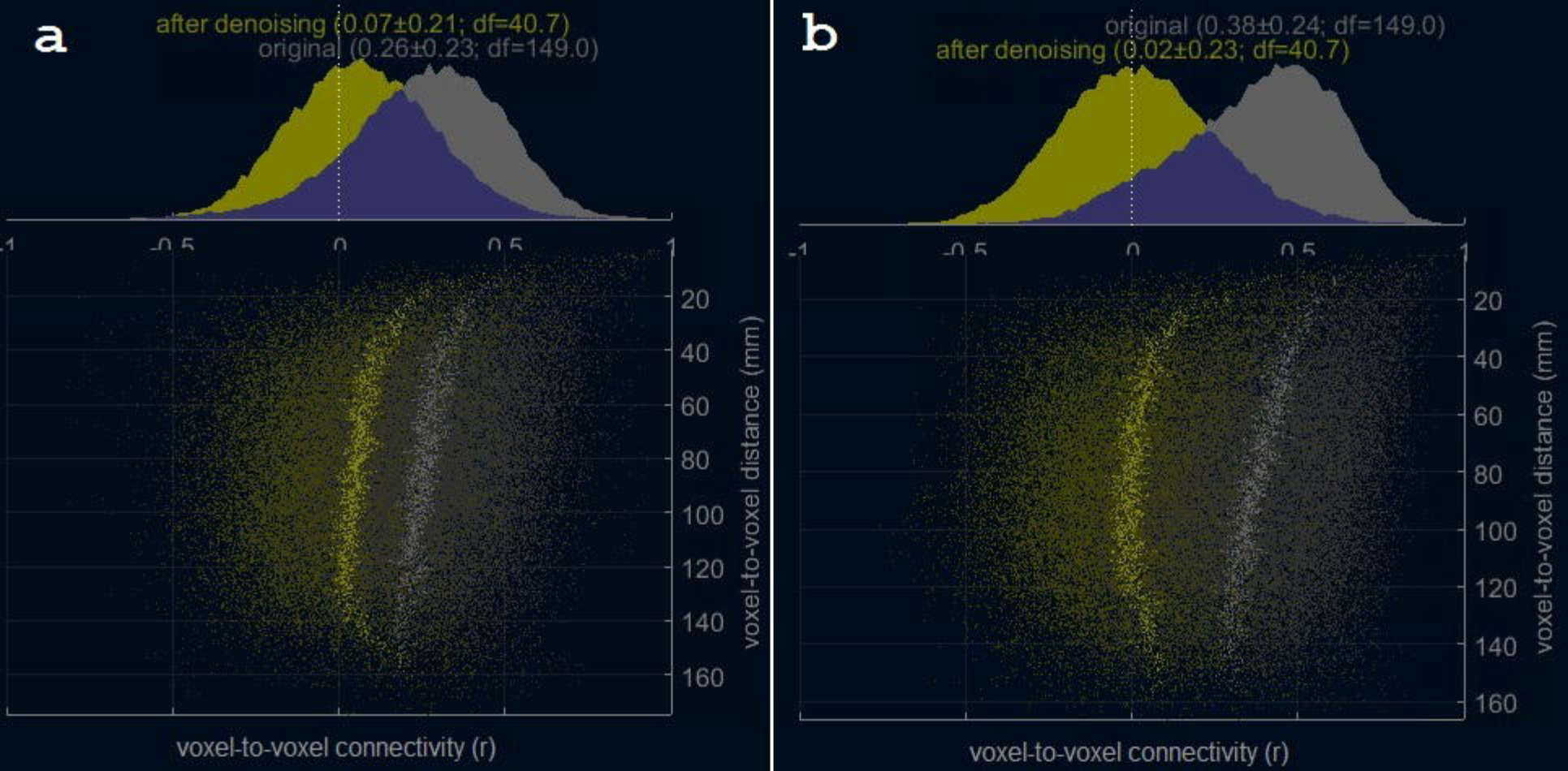
a
after denoising (0.07±0.21; df=40.7)
original (0.26±0.23; df=149.0)
-1
-0.5
0
0.5
1
20
40
60
80
100
120
140
160
voxel-to-voxel distance (mm)
voxel-to-voxel connectivity (r)
b
original (0.38±0.24; df=149.0)
after denoising (0.02±0.23; df=40.7)
-1
-0.5
0
0.5
1
20
40
60
80
100
120
140
160
voxel-to-voxel distance (mm)
voxel-to-voxel connectivity (r)

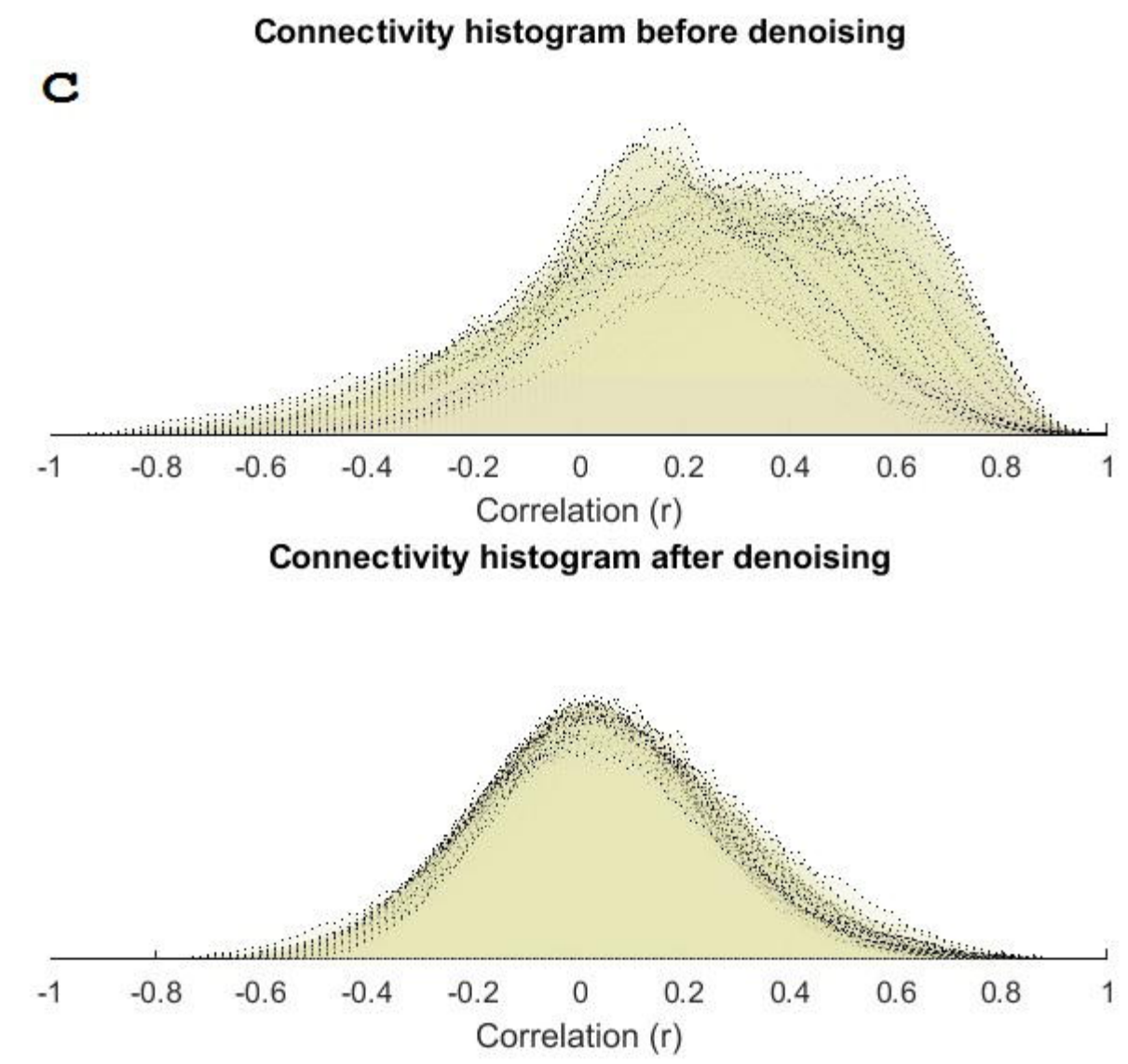
Connectivity histogram before denoising
C
-1
-0.8
-0.6
-0.4
-0.2
0
0.2
0.4
0.6
0.8
1
Correlation (r)
Connectivity histogram after denoising
-1
-0.8
-0.6
-0.4
-0.2
0
0.2
0.4
0.6
0.8
1
Correlation (r)

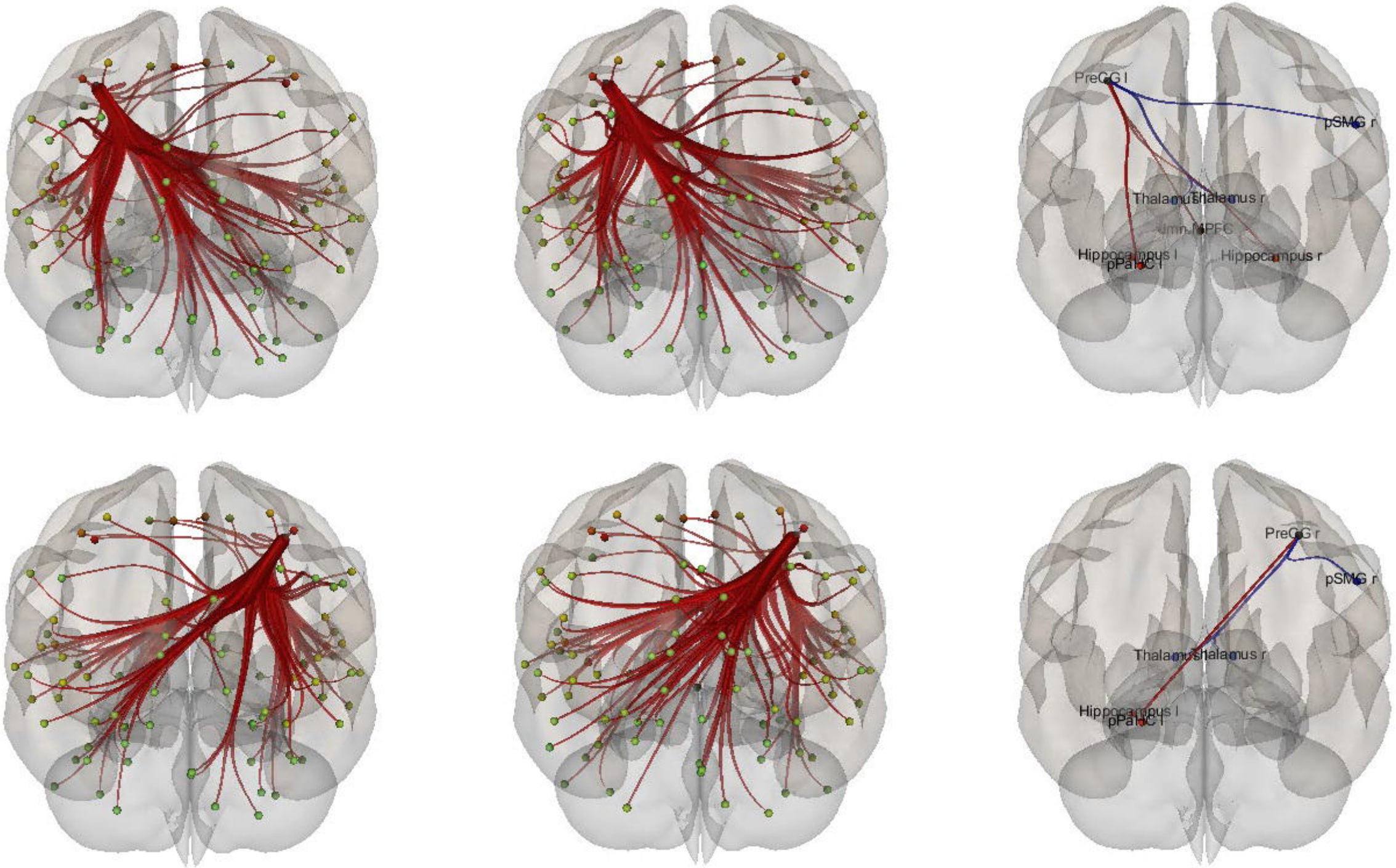
PreCG l
pSMG r
Thalamus l
Thalamus r
Hippocampus l
Hippocampus r
PreCG r
pSMG r
Thalamus l
Thalamus r
Hippocampus l

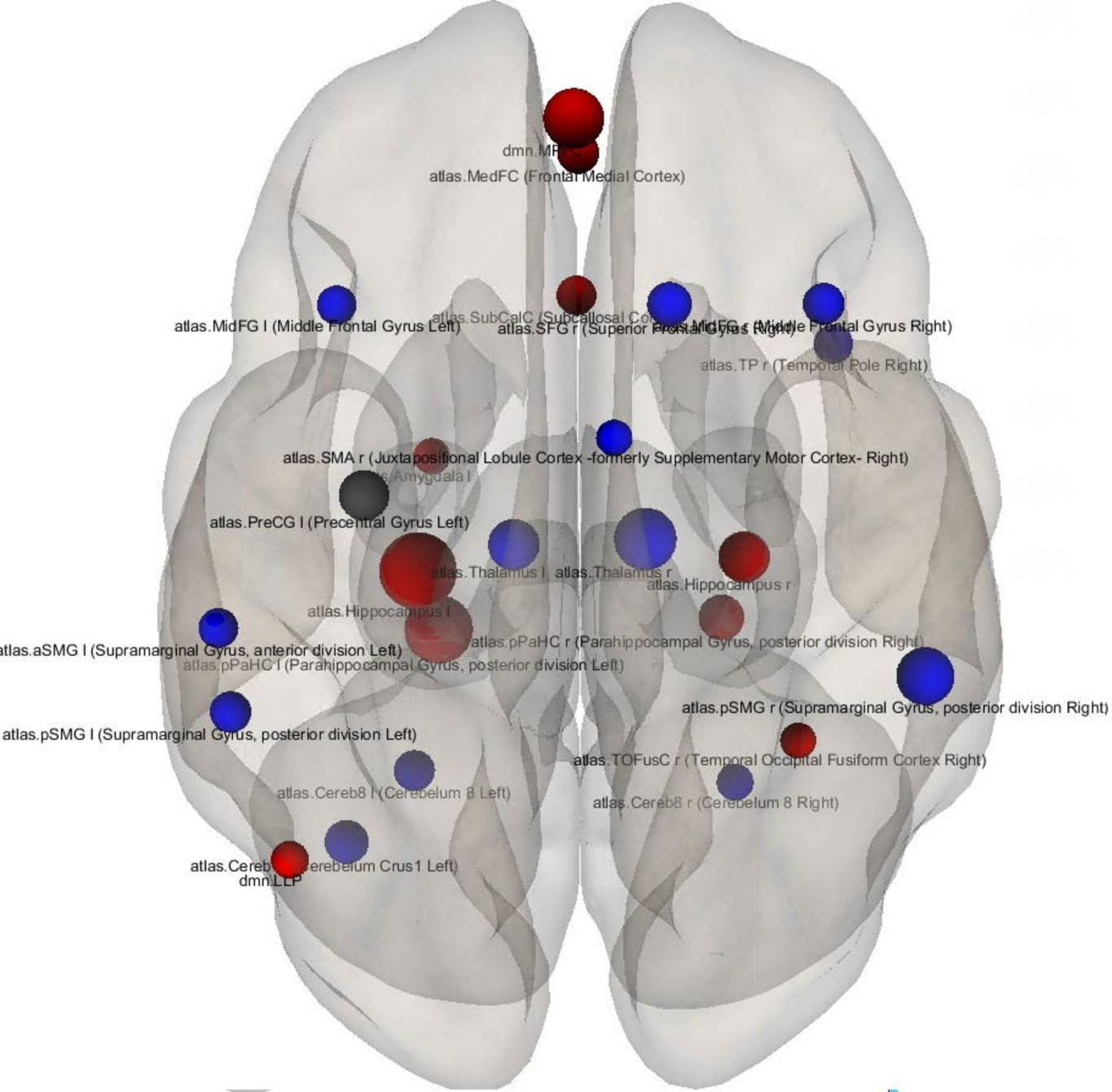
atlas.MedFC (Frontal Medial Cortex)
atlas.MidFG l (Middle Frontal Gyrus Left)
atlas.SFG r (Superior Frontal Gyrus Right)
atlas.TP r (Temporal Pole Right)
atlas.SMA r (Juxtapositional Lobule Cortex -formerly Supplementary Motor Cortex- Right)
atlas.PreCG l (Precentral Gyrus Left)
atlas.Thalamus l
atlas.Thalamus r
atlas.Hippocampus r
atlas.Hippocampus l
atlas.aSMG l (Supramarginal Gyrus, anterior division Left)
atlas.pPaHC r (Parahippocampal Gyrus, posterior division Right)
atlas.pPaHC l (Parahippocampal Gyrus, posterior division Left)
atlas.pSMG r (Supramarginal Gyrus, posterior division Right)
atlas.pSMG l (Supramarginal Gyrus, posterior division Left)
atlas.TOFusC r (Temporal Occipital Fusiform Cortex Right)
atlas.Cereb8 l (Cerebelum 8 Left)
atlas.Cereb8 r (Cerebelum 8 Right)
dmn.LLP

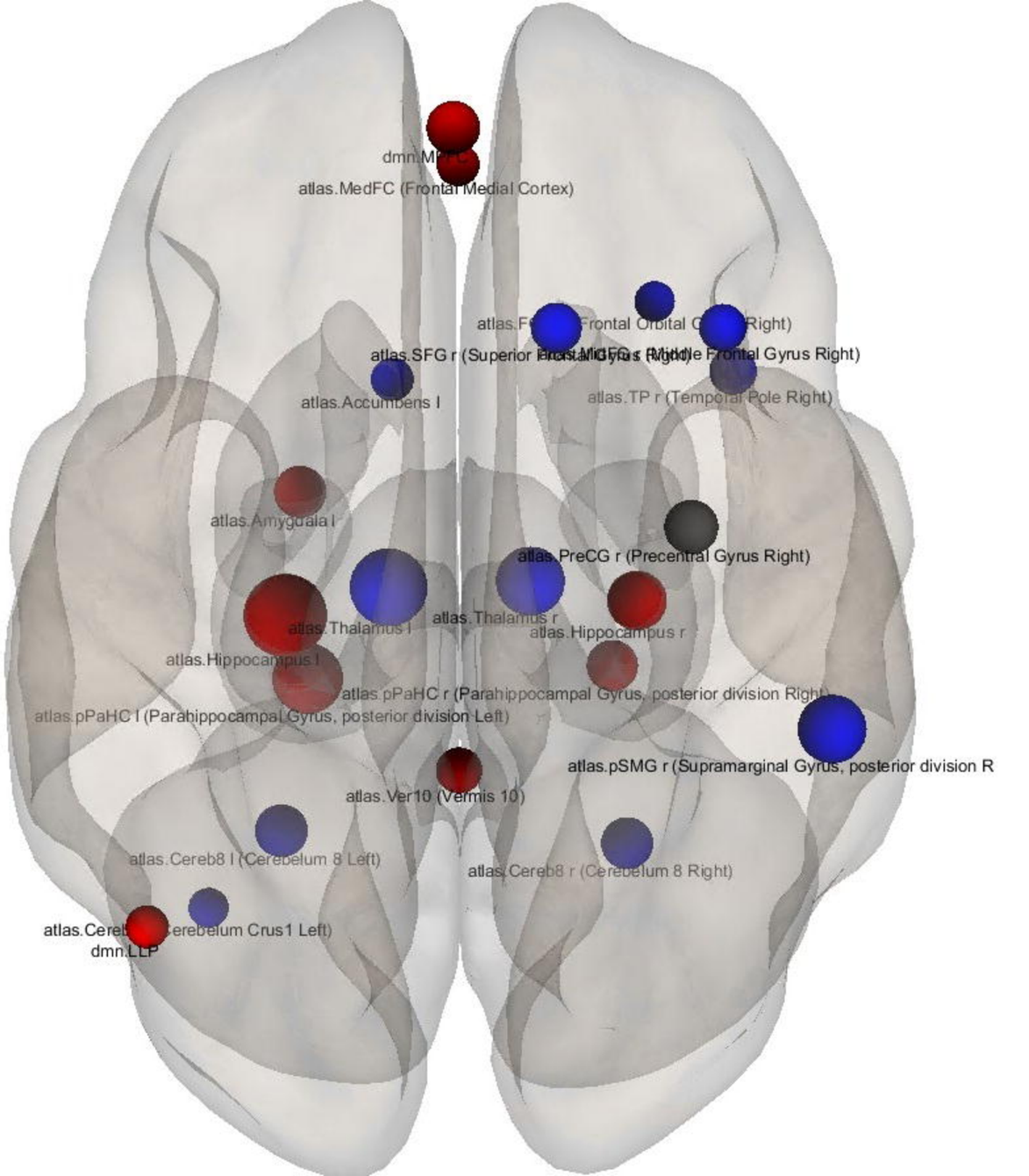
atlas.MedFC (Frontal Medial Cortex)
atlas.SFG r (Superior Frontal Gyrus Right)
atlas.Accumbens l
atlas.TP r (Temporal Pole Right)
atlas.Amygdala l
atlas.PreCG r (Precentral Gyrus Right)
atlas.Thalamus l
atlas.Thalamus r
atlas.Hippocampus r
atlas.Hippocampus l
atlas.pPaHC r (Parahippocampal Gyrus, posterior division Right)
atlas.pPaHC l (Parahippocampal Gyrus, posterior division Left)
atlas.pSMG r (Supramarginal Gyrus, posterior division R
atlas.Ver10 (Vermis 10)
atlas.Cereb8 l (Cerebelum 8 Left)
atlas.Cereb8 r (Cerebelum 8 Right)
dmn.LLP

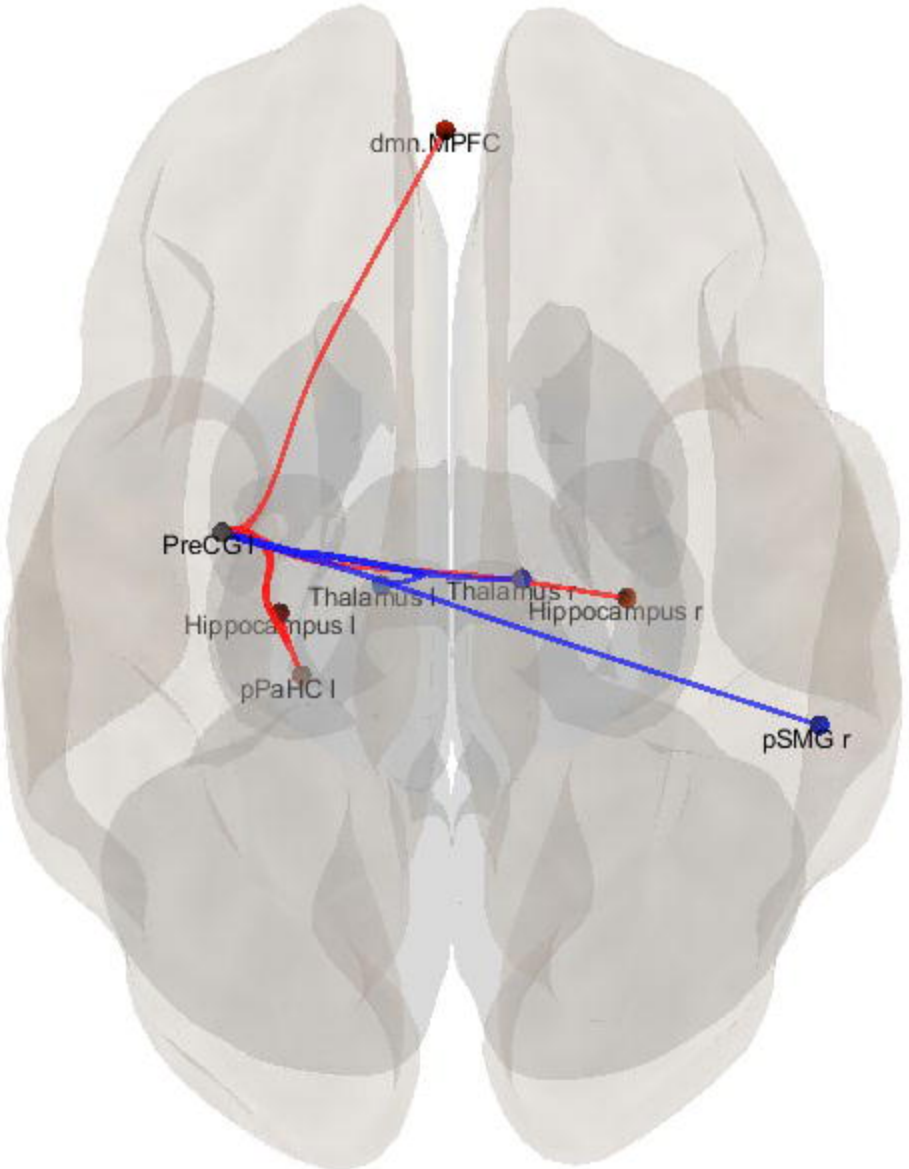
dmn.MPFC
PreCG l
Thalamus l
Thalamus r
Hippocampus r
Hippocampus l
pPaHC l
pSMG r

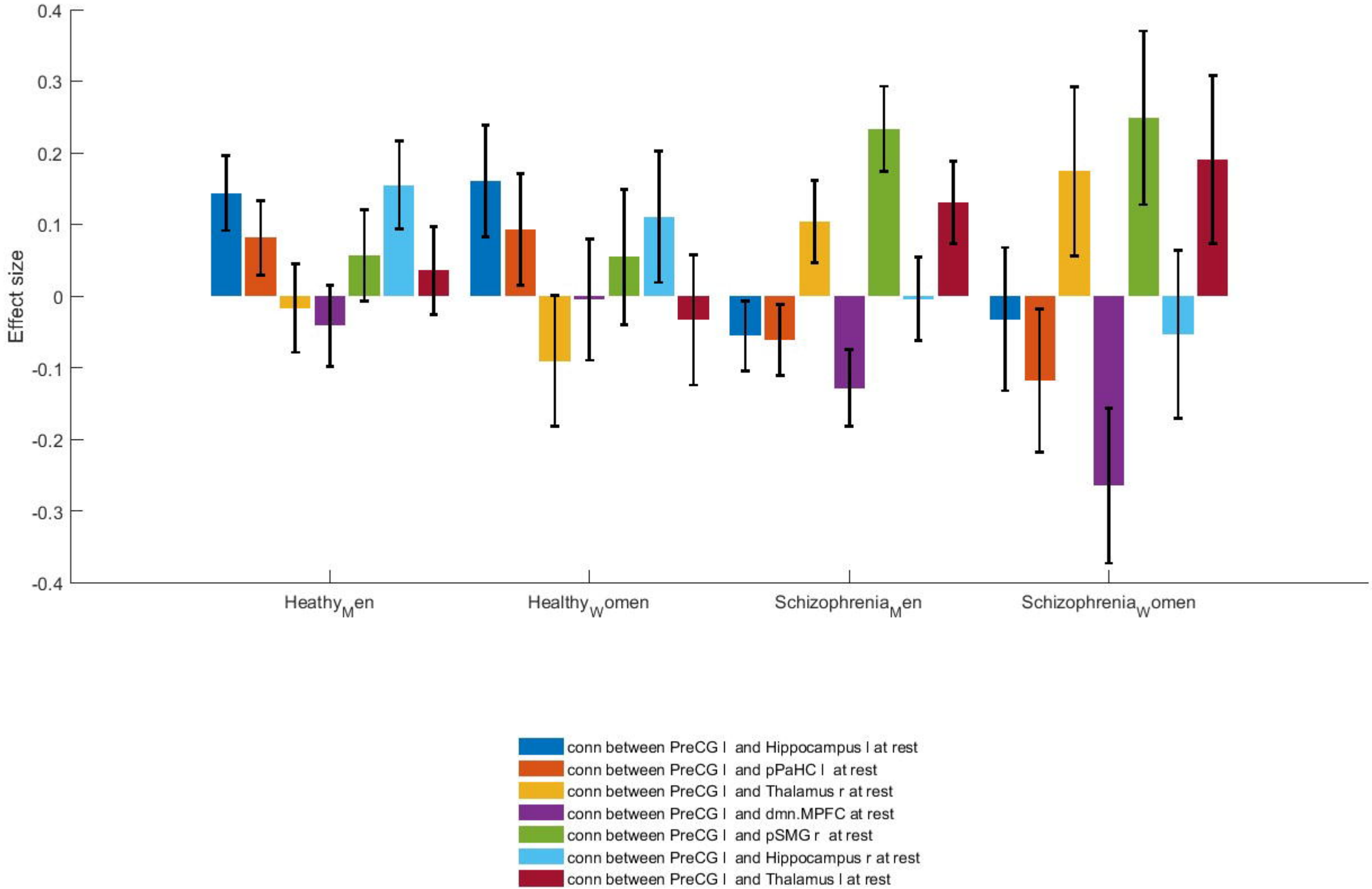
0.4
0.3
0.2
0.1
0
-0.1
-0.2
-0.3
-0.4
Effect size
Heathy_Men
Healthy_Women
Schizophrenia_Men
Schizophrenia_Women
conn between PreCG l and Hippocampus l at rest
conn between PreCG l and pPaHC l at rest
conn between PreCG l and Thalamus r at rest
conn between PreCG l and dmn.MPFC at rest
conn between PreCG l and pSMG r at rest
conn between PreCG l and Hippocampus r at rest
conn between PreCG l and Thalamus l at rest

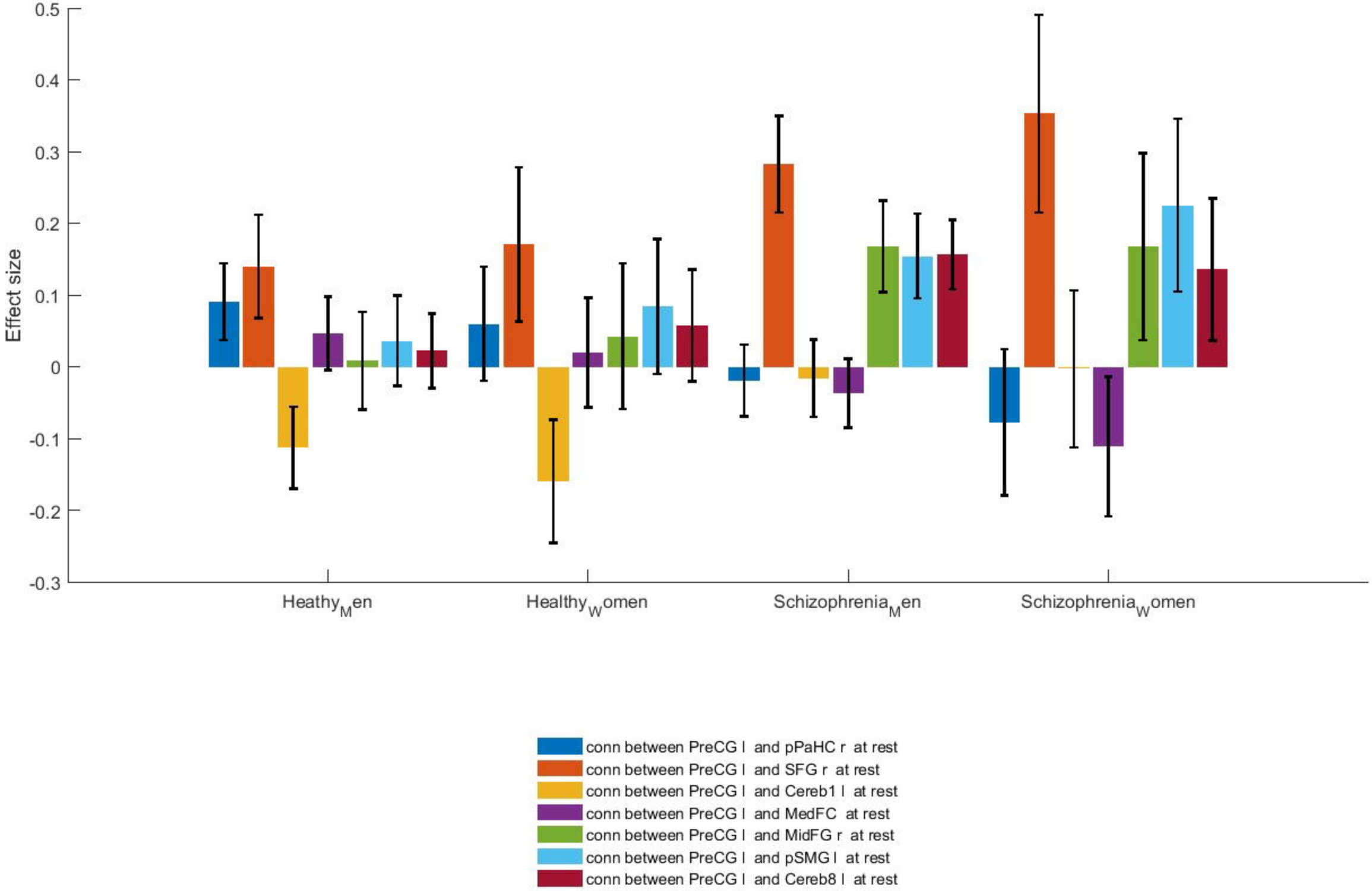
0.5
0.4
0.3
0.2
0.1
0
-0.1
-0.2
-0.3
Effect size
Heathy_Men
Healthy_Women
Schizophrenia_Men
Schizophrenia_Women
conn between PreCG l and pPaHC r at rest
conn between PreCG l and SFG r at rest
conn between PreCG l and Cereb1 l at rest
conn between PreCG l and MedFC at rest
conn between PreCG l and MidFG r at rest
conn between PreCG l and pSMG l at rest
conn between PreCG l and Cereb8 l at rest

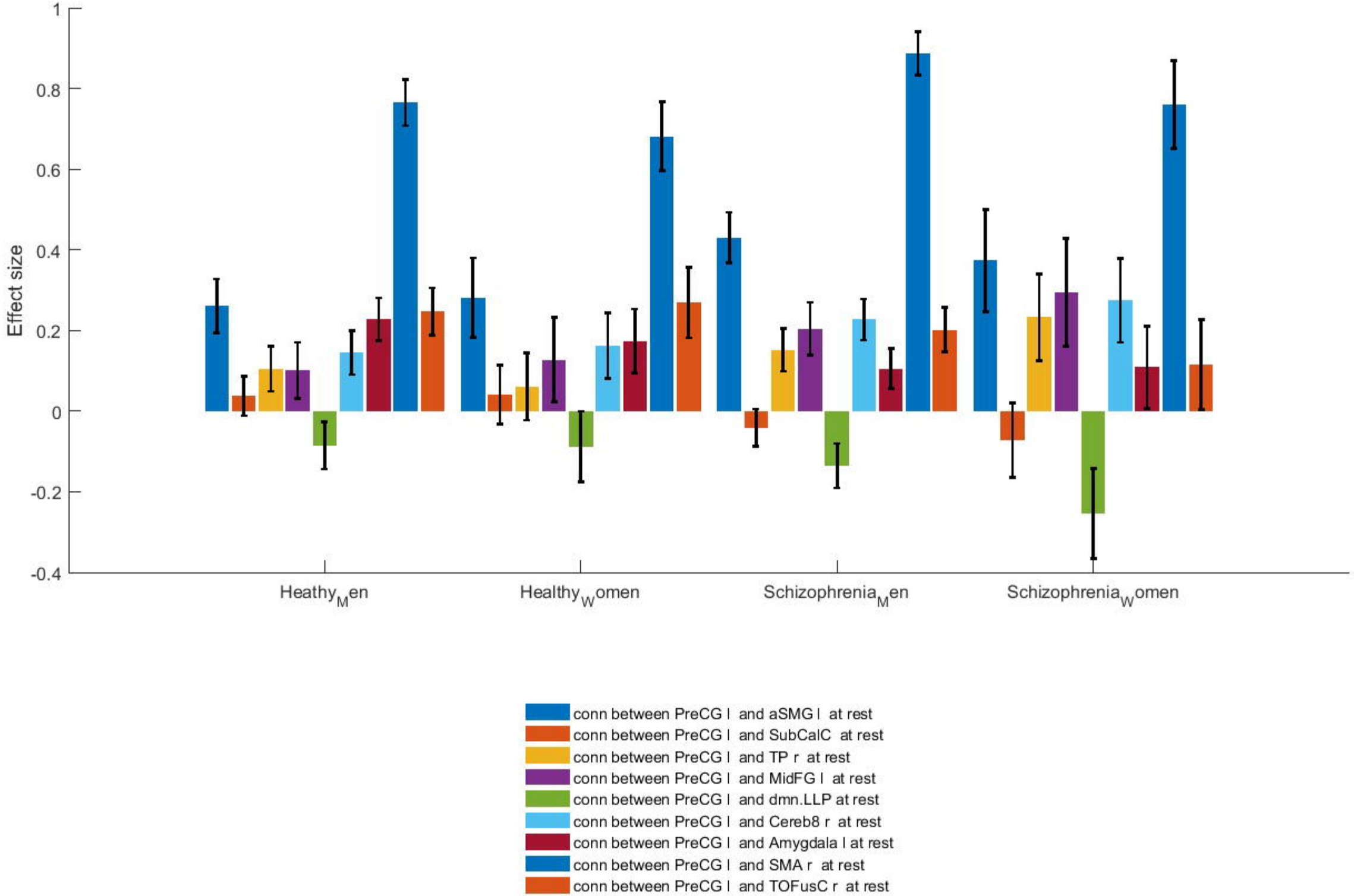
Effect size
1
0.8
0.6
0.4
0.2
0
-0.2
-0.4
Heathy_Men
Healthy_Women
Schizophrenia_Men
Schizophrenia_Women
conn between PreCG l and aSMG l at rest
conn between PreCG l and SubCalC at rest
conn between PreCG l and TP r at rest
conn between PreCG l and MidFG l at rest
conn between PreCG l and dmn.LLP at rest
conn between PreCG l and Cereb8 r at rest
conn between PreCG l and Amygdala l at rest
conn between PreCG l and SMA r at rest
conn between PreCG l and TOFusC r at rest

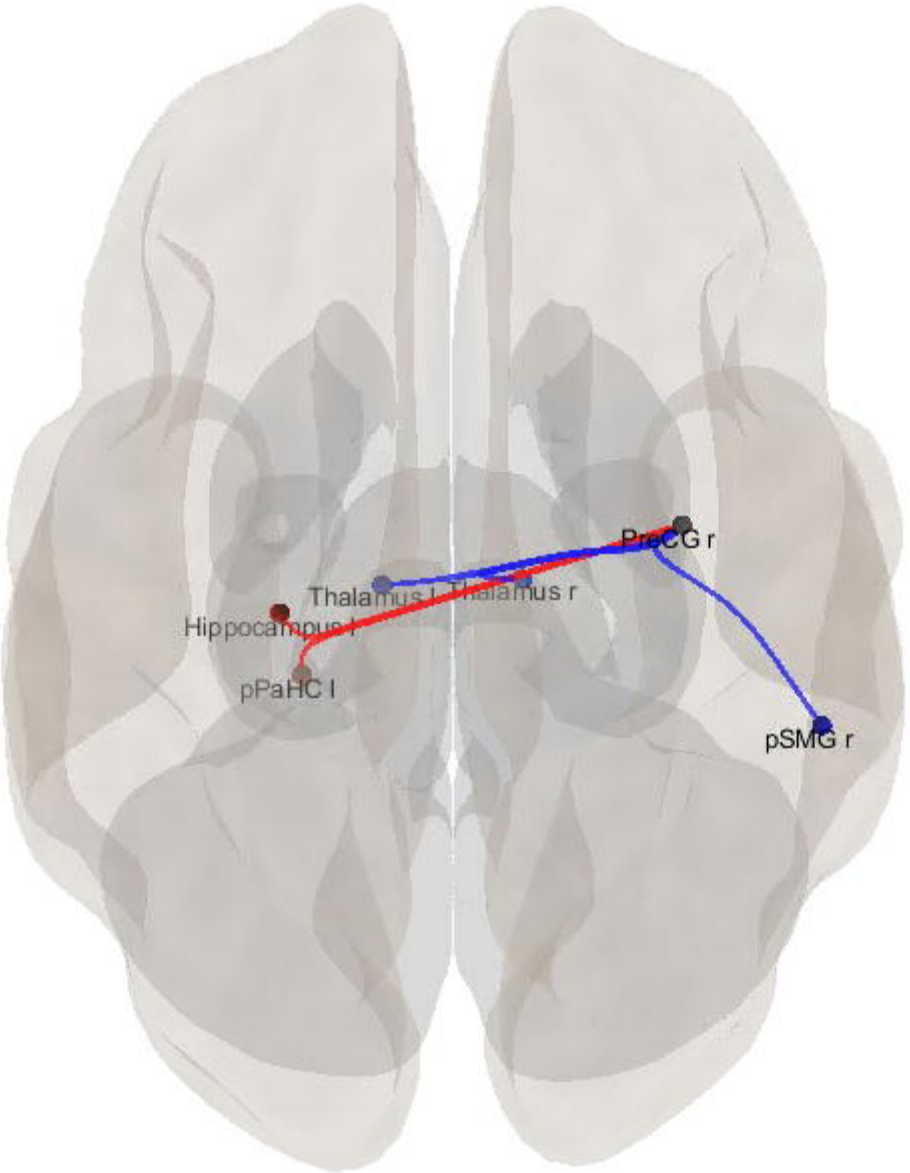
PreCG r
Thalamus l
Thalamus r
Hippocampus l
pPaHC l
pSMG r

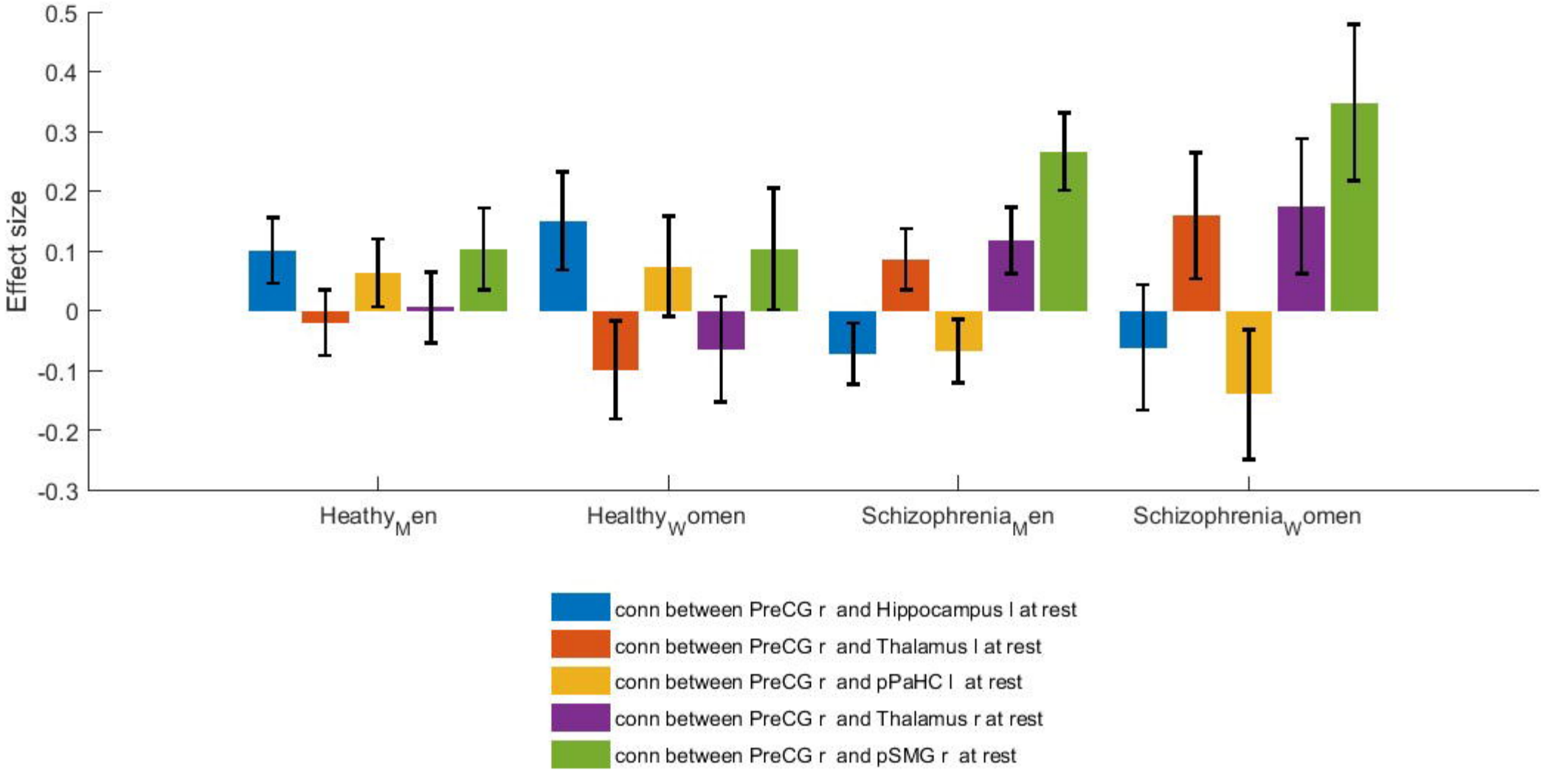
0.5
0.4
0.3
0.2
0.1
0
-0.1
-0.2
-0.3
Effect size
Heathy_Men
Healthy_Women
Schizophrenia_Men
Schizophrenia_Women
conn between PreCG r and Hippocampus l at rest
conn between PreCG r and Thalamus l at rest
conn between PreCG r and pPaHC l at rest
conn between PreCG r and Thalamus r at rest
conn between PreCG r and pSMG r at rest

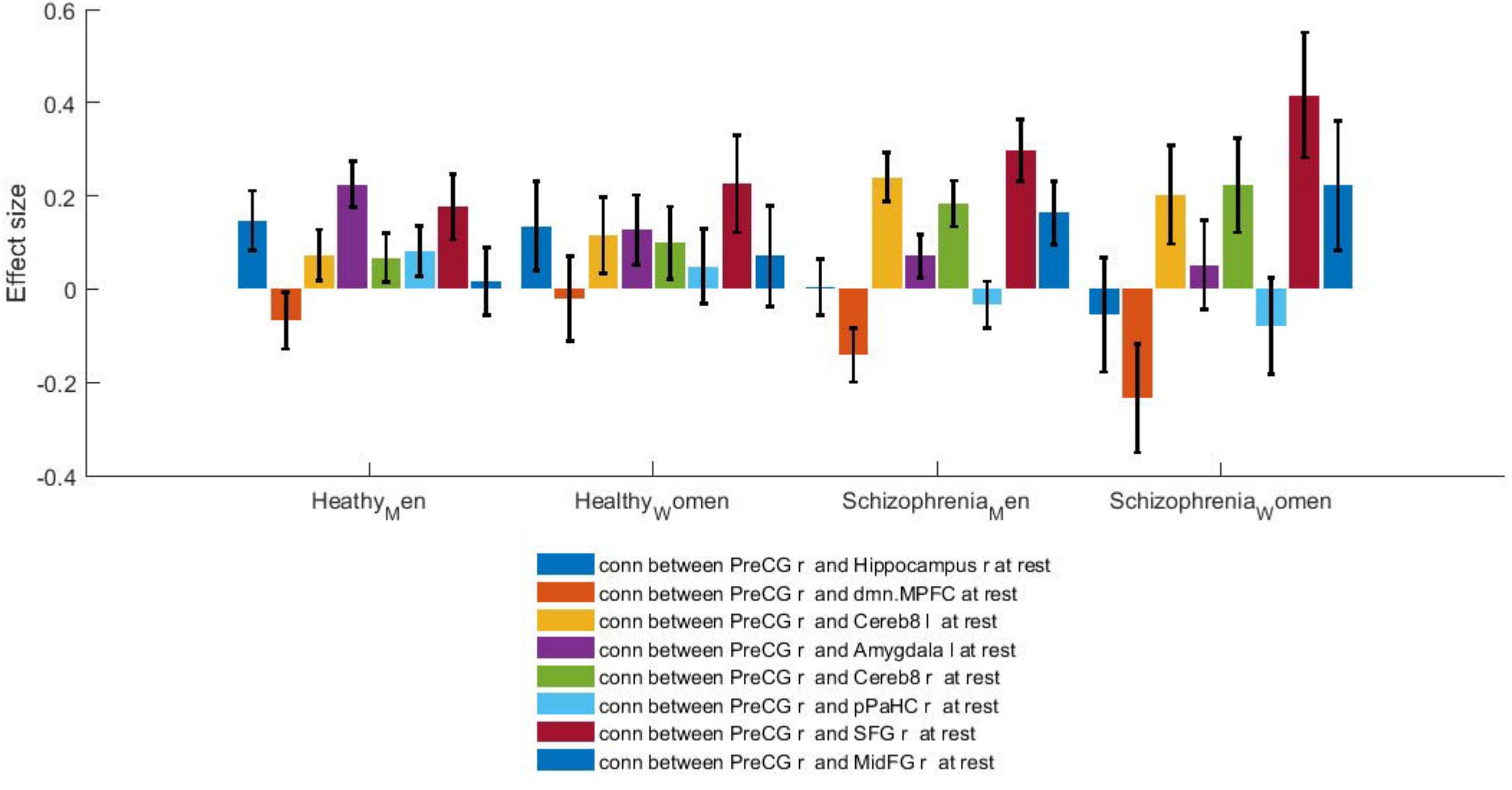
0.6
0.4
0.2
0
-0.2
-0.4
Effect size
Heathy_Men
Healthy_Women
Schizophrenia_Men
Schizophrenia_Women
conn between PreCG r and Hippocampus r at rest
conn between PreCG r and dmn.MPFC at rest
conn between PreCG r and Cereb8 l at rest
conn between PreCG r and Amygdala l at rest
conn between PreCG r and Cereb8 r at rest
conn between PreCG r and pPaHC r at rest
conn between PreCG r and SFG r at rest
conn between PreCG r and MidFG r at rest

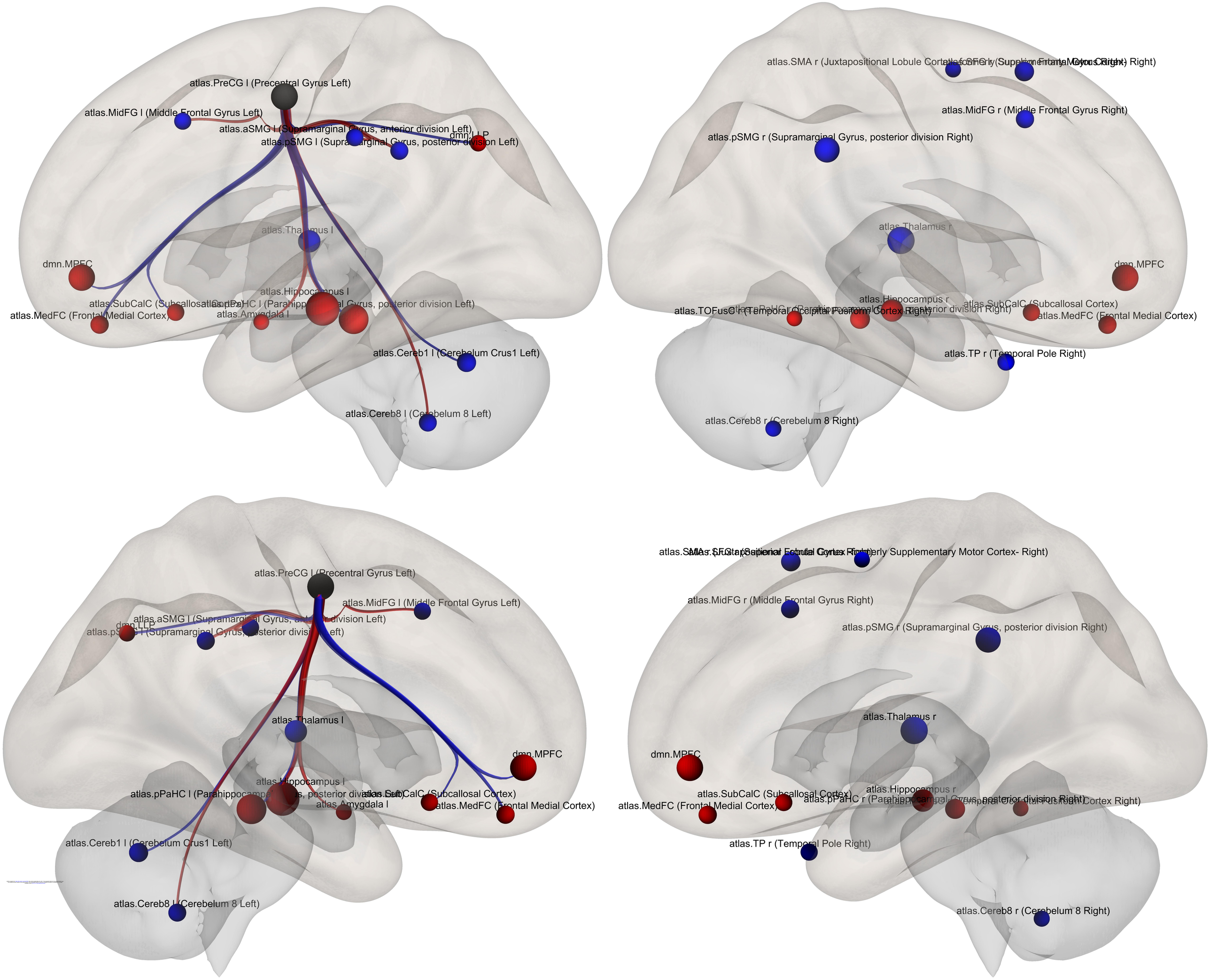
atlas.PreCG l (Precentral Gyrus Left)
atlas.MidFG l (Middle Frontal Gyrus Left)
atlas.aSMG l (Supramarginal Gyrus, anterior division Left)
dmn.LLP
atlas.pSMG l (Supramarginal Gyrus, posterior division Left)
atlas.Thalamus l
dmn.MPFC
atlas.Hippocampus l
atlas.SubCalC (Subcallosal Cortex)
atlas.MedFC (Frontal Medial Cortex)
atlas.Amygdala l
atlas.Cereb1 l (Cerebelum Crus1 Left)
atlas.Cereb8 l (Cerebelum 8 Left)
atlas.SMA r (Juxtapositional Lobule Cortex (formerly Supplementary Motor Cortex- Right)
atlas.MidFG r (Middle Frontal Gyrus Right)
atlas.pSMG r (Supramarginal Gyrus, posterior division Right)
atlas.Thalamus r
dmn.MPFC
atlas.Hippocampus r
atlas.SubCalC (Subcallosal Cortex)
atlas.MedFC (Frontal Medial Cortex)
atlas.TP r (Temporal Pole Right)
atlas.Cereb8 r (Cerebelum 8 Right)
atlas.PreCG l (Precentral Gyrus Left)
atlas.MidFG l (Middle Frontal Gyrus Left)
atlas.aSMG l (Supramarginal Gyrus, anterior division Left)
dmn.LLP
atlas.Thalamus l
dmn.MPFC
atlas.Hippocampus l
atlas.pPaHC l (Parahippocampal Gyrus, posterior division Left)
atlas.SubCalC (Subcallosal Cortex)
atlas.Amygdala l
atlas.MedFC (Frontal Medial Cortex)
atlas.Cereb1 l (Cerebelum Crus1 Left)
atlas.Cereb8 l (Cerebelum 8 Left)
atlas.MidFG r (Middle Frontal Gyrus Right)
atlas.pSMG r (Supramarginal Gyrus, posterior division Right)
atlas.Thalamus r
dmn.MPFC
atlas.SubCalC (Subcallosal Cortex)
atlas.Hippocampus r
atlas.pPaHC r (Parahippocampal Gyrus, posterior division Right)
atlas.MedFC (Frontal Medial Cortex)
atlas.TP r (Temporal Pole Right)
atlas.Cereb8 r (Cerebelum 8 Right)